ACS APPLIED MATERIALS & INTERFACES

Research Article

www.acsami.org

Hybrid Hairy Janus Particles Decorated with Metallic Nanoparticles for Catalytic Applications

Alina Kirillova,[†,‡] Christian Schliebe,[§] Georgi Stoychev,[†,‡] Alexander Jakob,[§] Heinrich Lang,*[,§] and Alla Synytska*[,†,‡]

[†]Leibniz-Institut für Polymerforschung Dresden e.V., Hohe Strasse 6, 01069 Dresden, Germany

[‡]Technische Universität Dresden, Physical Chemistry of Polymer Materials, 01062 Dresden, Germany

[§]Technische Universität Chemnitz, Faculty of Natural Sciences, Institute of Chemistry, Inorganic Chemistry, 09107 Chemnitz, Germany

Supporting Information

ABSTRACT: We report for the first time on the design of an advanced hairy hybrid Janus-type catalyst, which is comprised of an inorganic silica core covered with two distinct polymeric shells (hydrophilic and hydrophobic) on its opposite sides, while the catalytic species (in our case silver or gold nanoparticles) are immobilized directly into the hydrophilic stimuli-responsive polymer shell. The primary 200 nm large Janus particles with poly(acrylic acid) serving as the hydrophilic and polystyrene as the hydrophobic polymer were synthesized through a Pickering emulsion and a combination of "grafting from"/"grafting to" approaches. The incorporation of silver and gold nanoparticles within the hydrophilic polymer shell was achieved by infiltrating the respective metal ions into the polymer matrix, and nanoparticles were formed upon the addition of a reducing agent (triethylamine). Plasmon absorptions typical for silver and gold nanostructures were observed on the functionalized Janus particles using UV−vis spectroscopy. The respective systems were investigated by TEM and cryo-TEM revealing that the incorporated nanoparticles are selectively localized on the poly(acrylic acid) side of the Janus particles. The efficiency of the catalyst as well as the accessibility of the incorporated nanoparticles was tested on the reduction of Methylene Blue, Eosin Y, and 4-nitrophenol as convenient benchmark systems. Ultimately, the hairy Janus particles with immobilized Ag or Au nanoparticles efficiently catalyzed the respective reactions by applying extremely low amounts of catalyst. Finally, we demonstrated several advantages of the use of JPs with immobilized metallic nanoparticles, which are (i) JPs stabilize the emulsions, (ii) the emulsion can be destabilized by utilizing responsive properties of the JPs, and (iii) JPs can easily be recovered after reaction and reused again.

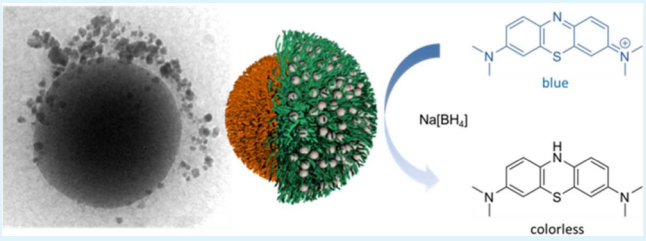

KEYWORDS: *Janus particles, hybrid hairy Janus particles, stimuli-responsive Janus particles, silver and gold nanoparticles, interfacial catalysis, catalysis, efficient catalyst*

1. INTRODUCTION

Anisotropic particles have attracted attention in recent years due to their advanced morphologies and numerous potential applications, ranging from electronics to sensing, nanomedicine, or catalysis.[1−4] Janus particles (JPs) are a unique class among such asymmetric nano/microobjects, comprising two distinct functionalities in one small particle. Named after the two-faced Roman god Janus, these particles exhibit unique multifunctionality and resemblance to molecular amphiphiles, such as surfactants, phospholipids, and block copolymers, which makes them attractive novel units for self-assembly of complex structures, drug delivery, display technology, catalysis, etc.[5−7]

Recently, nanocatalysts with advanced tunable architectures of different sizes and compositions have attracted significant attention.[4,8,9] Consequently, the Janus geometry could be applied to the catalysts to provide them with a higher and thus sufficient level of heterogeneity required to address the problems of stability, recovery, reuse, etc. The spatial isolation of catalytic species on a JP could provide direct access to reactants and hence opens new paths in the field of interfacial and simultaneous catalysis.

Janus geometries have already been previously used for the design of novel solid catalysts.[10−12] Considering that the presence of a metallic component in JPs can provide them with the desired catalytic properties, several examples of anisotropic particles have been reported as catalysts, mainly in the area of photocatalysis.[13] Pradhan et al. have highlighted the photocatalytic activity of Au-TiO_2 snowman-like heterodimers in the oxidation of methanol to formaldehyde in the presence of light,[14] whereas Seh et al. reported the use of Au-TiO_2

Received: June 12, 2015
Accepted: September 11, 2015
Published: September 11, 2015

DOI: 10.1021/acsami.5b05224
ACS Appl. Mater. Interfaces 2015, 7, 21218−21225

photocatalysts for efficient visible-light H_2 generation from an aqueous isopropyl alcohol solution.[15]

The concept of Janus-type solid catalysts is particularly advantageous in the field of interfacial catalysis due to the high interfacial energy and thus excellent emulsion-stabilizing properties of the Janus particles.[16,17] Another advantage is an easy recovery of such catalysts from the reaction mixtures, which makes them recyclable. Additionally, high interfacial area provided by JPs can facilitate better conversion and mass transfer between phases.

Previously, it was shown that carbon nanohybrids can be successfully used as solid catalysts for reactions carried out in aqueous/organic emulsions.[4] For instance, Resasco and co-workers have demonstrated the ability of solid hybrid Janus-type catalysts to catalyze reactions at the water−oil interface.[18] Their catalysts were hybrid nanoparticles (NPs) consisting of carbon nanotubes fused to silica, which were made catalytically active by depositing a transition metal such as Pd onto them. Promising results were obtained for several reactions relevant to biofuel refining, thus, indicating the importance of such solid particle catalysts that are able to simultaneously stabilize emulsions. They have further extended their catalyst library by preparing other Janus-type interfacial catalysts by hydrophobizing one side of fumed silica NPs with aminopropyltriethoxysilane (APTES).[19]

Another example of a heterogeneous catalyst system was produced by Lahann and co-workers.[20] They have synthesized inorganic JPs through electrohydrodynamic (EHD) cojetting, utilizing a degradable templating polymer. In the final architecture, catalytic nanocrystals were localized in only one hemisphere of the spherical JPs, enabling subsequent growth of MWCNTs in a spatially controlled manner.

Despite the diversity of JPs used for catalytic applications, it must be noted that all of the above-mentioned examples consider the so-called "bare" JPs, that is, particles that do not have "hairy" polymer shells (or polymers, for that matter) involved in their final design. Nevertheless, the role of the polymer could be very important in the creation of novel hybrid Janus catalysts. First, polymer shells with a high contrast in hydrophobicity on the opposite sides of the JPs would increase their affinity toward different phases (e.g., oil and water) in an emulsion (interfacial catalysis) thus, stabilizing it to a higher extent than the corresponding bare particles.[21] Second, the "hairy" polymeric architectures and their ability to swell and deswell could provide a better distribution of the catalytic NP species throughout the catalyst surface and hence allow better substance transport to the catalyst and higher reaction rates. Third, stimuli-responsive polymers can be used as shells, which would allow a great extent of control over the reaction, for example, inducing or, on the contrary, blocking the catalytic activity would be possible upon external stimuli. Finally, if grafted to an inorganic core, polymer shells would increase the complexity of the Janus catalyst, making its architecture well-defined, hybrid, and robust, thus, providing the catalyst with a high level of heterogeneity required for successful heterogeneous catalysis.

Therefore, we report on the design of an advanced "hairy" hybrid Janus-type catalyst, which comprises an inorganic silica core covered with two distinct polymeric shells (hydrophilic and hydrophobic) on its opposite sides, while the catalytic species (in our case silver or gold NPs) are immobilized directly into the hydrophilic stimuli-responsive polymer shell. The role of the hydrophilic polymer is to ensure a homogeneous distribution of the NPs throughout its hairy chains upon swelling in water thus providing better substance transport possibilities. On the other hand, the role of the hydrophobic polymer is to provide the catalyst with amphiphilicity and to alleviate its use for interfacial catalysis. The prepared hairy hybrid JP-NP complex is directly visualized through TEM and cryo-TEM. Furthermore, its catalytic performance is tested by applying it in several benchmark reactions, such as the reduction of Methylene Blue, Eosin Y, and 4-nitrophenol.

2. EXPERIMENTAL SECTION

Materials. Tetraethylorthosilicate (TEOS, 99%, Fluka), ammonia solution (NH_4OH, 28−30% solution, Acros), ethanol abs. (EtOH, 99.9%, VWR), 3-aminopropyltriethoxysilane (APS, 97%, ABCR), paraffin wax (mp. 53−57 °C, Aldrich), α-bromoisobutyric acid (BiBA, 98%, Aldrich), *N*-(3-(dimethylamino)propyl)-*N*′-ethylcarbodiimide hydrochloride (EDC, Aldrich), *N*-hydroxysuccinimide (NHS, Aldrich), hexane (95%, Aldrich), dichloromethane (>99%, Acros), copper(II) bromide (99.999%, Aldrich), tin(II) 2-ethylhexanoate (95%, Aldrich), *N*,*N*,*N*′,*N*″,*N*″-pentamethyldiethylenetriamine (PMDTA, 99%, Aldrich), ethyl α-bromoisobutyrate (EBiB, 98%; Aldrich), toluene (99.8%, Aldrich), chloroform (99.8%, Aldrich), tetrahydrofuran (>99%, Acros), methanesulfonic acid (99.5%, Aldrich), diethyl ether (99.7%, Aldrich), *tert*-butyl acrylate (tBA, 98%, Aldrich; was passed prior to polymerization through basic, neutral, and acidic aluminum oxides), $AgNO_3$ (Aldrich), $H[AuCl_4]$ (Aldrich), triethylamine (Aldrich), 4-nitrophenol (Aldrich), Methylene Blue (Aldrich), Eosin Y (Aldrich), and polystyrene (carboxy terminated, M_n, 50 400 g/mol; Polymer Source) were used as received.

Transmission Electron Microscopy (TEM) and Cryo-TEM. Transmission electron microscopy (TEM) images and cryogenic TEM images were taken with a Libra 120 cryo-TEM from Carl Zeiss NTS GmbH equipped with a LaB_6 source. The acceleration voltage was 120 kV and the energy filter with an energy window of 15 eV was used. Samples for TEM were prepared by immersing a TEM grid in a dispersion of PAA/PS-NP-JP for 20 s and removing excess liquid afterward with filter paper. Gold grids with a carbon film (300 mesh, CF300-Au-50) were used for the analysis (Electron Microscopy Sciences).

The 200 nm PAA/NH_2-JP sample for cryo-TEM was prepared as follows: JPs were dispersed in water (0.5 mg/mL) by ultrasonication for 20 min; pH 10 was adjusted to yield a swollen PAA shell. Prior to the analysis, 3.5 μL of the sample was taken, blotted, and vitrified in liquid ethane at −178 °C. Ultimately, an approximately 200 nm thick ice film was examined in the TEM. Cryo-TEM was used for the visualization and estimation of the thickness of polymer brushes. Statistical image analysis of different particles (approximately 30 particles) resulted in a brush thickness of 50 ± 10 nm for the swollen PAA polymer at pH 10. PAA/PS-NP-JP were also investigated with cryo-TEM under similar conditions.

Energy-Dispersive X-ray Spectroscopy/SEM. The elemental maps of the particles suspended on a TEM grid were acquired with a scanning electron microscope (SEM) Ultra 55 (Carl Zeiss Microscopy GmbH, Oberkochen, Germany) equipped with a Quantax XFlash 5060 energy dispersive X-ray (EDX) spectrometer (Bruker Corporation, Billerica, MA). The SEM was operated at an acceleration voltage of 6 kV, and a transmitted electron (TE) detector was used for imaging.

UV−Visible Spectroscopy. UV−vis spectroscopy was performed with Thermo Genesis 6 equipment using standard quartz glass vials with an optical path of 1 cm.

Synthesis of Monodisperse SiO_2 Particles. The 200 nm sized silica particles were synthesized using a multistep hydrolysis−condensation procedure of TEOS in an ammonia hydroxide−ethanol solution based on the Stöber approach.[22] In this respect, TEOS was added via a syringe into a mixture of ethanol and ammonia. The 100 nm large SiO_2 particles produced within the first step of synthesis were used as seeds for the next step. In the following step, 200 nm large

DOI: 10.1021/acsami.5b05224
ACS Appl. Mater. Interfaces 2015, 7, 21218−21225

SiO_2 particles were produced. Each reaction was carried out by stirring the mixture at 500 rpm overnight at ambient temperature. Subsequently, 200 nm large particles were separated from the dispersion by centrifugation and were purified with ethanol. Purified particles were dried in a vacuum oven under reduced pressure at 60 °C.

Synthesis of Bicomponent Polymeric JPs (PAA/PS-JP). Preparation of colloidosomes was done by a wax-water Pickering emulsion approach described elsewhere.[23,24] Colloidosomes were prepared with 200 nm APS-modified silica spheres. The ATRP-initiator was then immobilized onto the exposed particle surface.[25] Afterward, the modified colloidosomes were filtered off and washed with deionized water to remove unattached particles and the obtained material was dried in a vacuum oven at 25 °C overnight. Ultimately, the wax was dissolved in hexane, and the initiator-covered particles were used for polymerization.

Grafting of PtBA Using Surface-Initiated ATRP. Poly(*tert*-butyl acrylate) (PtBA) was grafted on the initiator-modified particles as follows: 5 mL of *tert*-butyl acrylate, 70 μL of PMDTA (0.5 M solution in DMF), 70 μL of $CuBr_2$ (0.1 M solution in DMF), and 0.15 μL of EBiB were added to the particles. The mixture was sonicated and purged with Ar, followed by the injection of 130 μL of tin(II) 2-ethylhexanoate. The polymerization was performed by placing the respective mixture in an oil bath under continuous stirring at 115 °C for 2 h. Afterward, the particles with the grafted polymer were washed by centrifugation in chloroform and toluene 8 times and were then dried in vacuum at 60 °C. Subsequently, PtBA was hydrolyzed with methanesulfonic acid to yield poly(acrylic acid) (PAA).

Grafting of Carboxy Terminated PS Using the "Grafting to" Approach. The "grafting to" approach was utilized to graft carboxy terminated polystyrene (PS-COOH) onto PAA/NH_2-JP containing amino groups.[23] For this purpose, the particles were dispersed in 20 mL of a 1 wt % solution of polystyrene and stirred for 2 h at ambient temprature. Next, the solvent was evaporated and the particles were annealed at 150 °C overnight (12 h). The ungrafted polymer was removed by eight cycles of particle redispersion in tetrahydrofuran and subsequent centrifugation. The acquired and purified PAA/PS-JP were ultimately dried in a vacuum oven at 40 °C.

General Procedure for the Incorporation of Metal Nanoparticles. In a typical procedure, 40 mg of the prepared PAA/PS-JP was dispersed in 40 mL of deionized water and sonicated for 10 min. The suspension was left to swell for an additional 48 h. Afterward, the mixture was placed in an ultrasonic bath for 5 min, 5 mL of a 10 mM $AgNO_3$ aqueous solution (5 mM solution was used in the case of $H[AuCl_4]$) was added in a single portion, and stirring was continued for 5 min. Next, 1 mL of triethylamine was added to the mixture in a single portion, which caused the suspension to change its color from colorless to brown (Ag) or deep violet (Au). Upon the addition of triethylamine, metal ions were reduced, and the respective nanoparticles (Ag or Au NPs) were formed and stabilized within the PAA part of the PAA/PS-JP. The reaction mixture was stirred for 12 h and was then centrifuged (5000 rpm, 20 min). The supernatant colored solution was discarded and the remaining solid was washed with deionized water (10 mL) and centrifuged again. Then the remaining solid was dispersed in 40 mL of water. This suspension was further used for the catalytic experiments.

General Procedure for the Catalytic Reduction of Dyes. A volume of 0.25 mL of the Ag-functionalized PAA/PS-JP suspension was added to a mixture of 40 mL of the specific dye (Methylene Blue or Eosin Y) 10^{-5} M aqueous solution and 2 mL of freshly prepared aqueous sodium borohydride (0.1 M) solution. Immediately after the addition, samples were taken each minute and analyzed by UV–vis spectroscopy, until the measured absorbance reached a constant value.

General Procedure for the Catalytic Reduction of 4-Nitrophenol. The appropriate reactions were performed in the same manner as for the dye reduction experiments stated above using the Au-functionalized PAA/PS-JP suspension at a temperature of 40 °C.

3. RESULTS AND DISCUSSION

Synthesis of Hairy Hybrid PAA/PS-JP. Janus particles (JPs) with a core diameter of 200 nm and a shell consisting of two polymers, poly(acrylic acid) (PAA) and polystyrene (PS) on the opposite sides of the particle were synthesized through a combination of "grafting from" and "grafting to" approaches as described elsewhere.[23,24] After grafting the first polymer (PAA) onto the modified silica particles, the monocomponent JPs were characterized by cryo-TEM. It can be clearly seen from the images (Figure 1) that the particles have a Janus character,

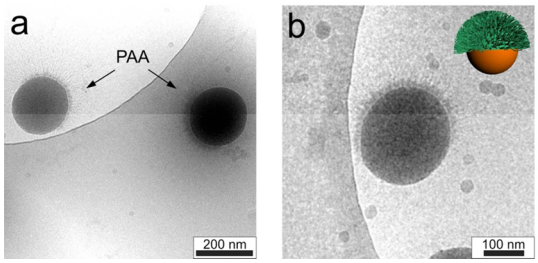

Figure 1. Representative cryo-TEM images at different magnifications of the synthesized 200 nm large hairy PAA/NH_2-JP: (a) two representative polymer-decorated Janus particles and (b) close-up image of one polymer-decorated Janus particle.

that is, PAA was selectively grafted onto one side of the silica particles. PAA/NH_2-JP particles were investigated at a high pH value (pH 10) to ensure the swelling and better visualization of the PAA polymer chains. The thickness of the swollen PAA layer at pH 10 was found to be 50 ± 10 nm. It was also concluded that the particles mostly have a 1:1 Janus ratio (area covered with PAA–area covered with PS). The grafting density of the polymer chains on the silica particle surface obtained from thermogravimetric analysis (TGA) and gel permeation chromatography (GPC) results is 0.2–0.3 chains/nm^2.

Modification of JPs with Metal Nanoparticles. Metal nanoparticles (Ag and Au NPs) were selectively immobilized into the PAA shell of the PAA/PS-JP and the resulting hybrid JP-NP systems were subsequently used to catalyze different reactions (Figure 2).

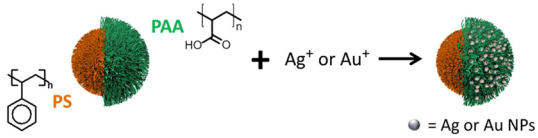

Figure 2. Scheme of the selective NP immobilization onto PAA/PS-JP for catalytic applications.

The prepared 200 nm PAA/PS-JP were immersed in deionized water and left to swell for 48 h. After that the particles were again redispersed by sonication and treated with 10 or 5 mM solutions of the respective metal source ($AgNO_3$ or $H[AuCl_4]$). Triethylamine was added to this mixture, which initiated the reduction process, as indicated by a color change from colorless to brown (silver) or dark violet (gold). The suspensions were stirred for 12 h and then the metal NP-functionalized JPs were separated by centrifugation, washed, and redispersed in water (see the Experimental Section for a more detailed procedure).

Broad absorption bands at 432 and 533 nm were observed, which are characteristic for the plasmon resonance of silver and

DOI: 10.1021/acsami.5b05224
ACS Appl. Mater. Interfaces 2015, 7, 21218–21225

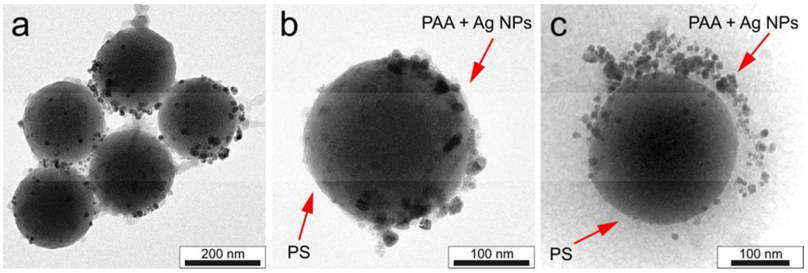

Figure 3. Characterization of hairy hybrid Janus catalysts: representative TEM (a, b) and cryo-TEM (c) images of PAA/PS-JP with selectively immobilized Ag NPs into the PAA shell. More representative cryo-TEM images, images of immobilized Au NPs, and the derived particle size distribution of the incorporated NPs can be found in the Supporting Information (Figures S2−S4). Results on the EDX analysis of PAA/PS-Ag-JP and PAA/PS-Au-JP systems are presented in Figure 4 and Figure S6.

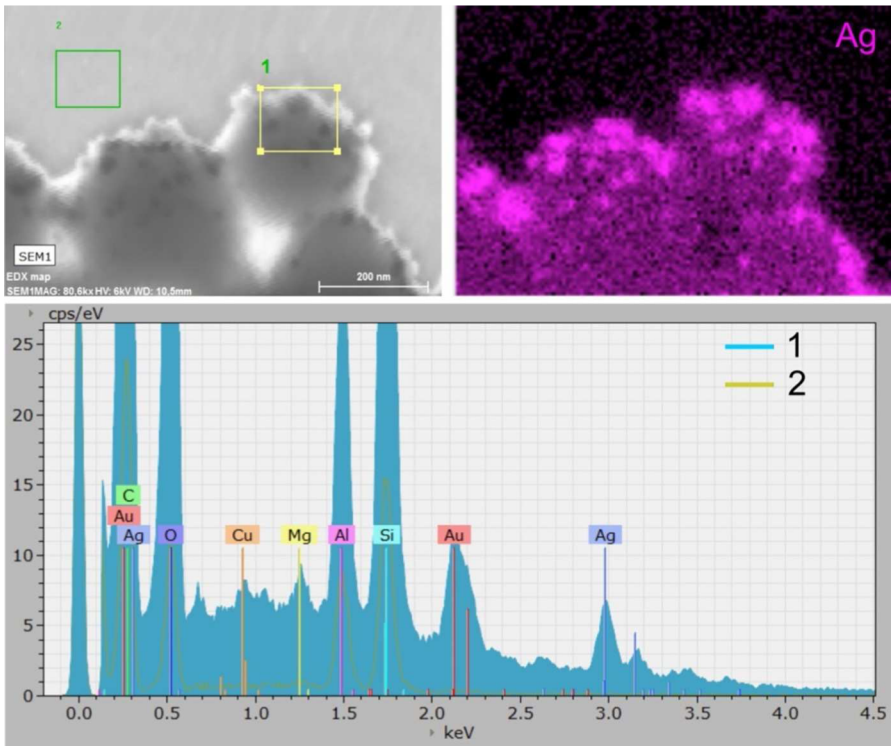

Figure 4. EDX analysis of PAA/PS-Ag-JP. Upper left panel, STEM image of the particles; upper right, Ag mapping; lower panel, EDX spectrum of areas 1 and 2. EDX analysis of PAA/PS-Au-JP is displayed in Figure S6.

gold NPs (Figure S1),[26−29] respectively, and therefore, indicate the successful formation of these nanostructures.

Characterization of the Modified JPs. The formation of metal NPs on the PAA/PS-JP was confirmed by transmission electron microscopy (TEM) measurements (Figure 3a,b; Figure S2). Considering the obtained images, the formation of NPs with mean diameters of 12 ± 4 nm for Ag and 15 ± 6 nm for Au was observed (Figure S2). A broad particle size distribution was characteristic for both metals, which can be attributed to the diffusion of further metal ions from the surrounding solution through the swollen polymer and has been observed for similar polymeric stabilizers as well.[30,31]

Additionally, TEM images revealed selective localization of the corresponding NPs in the PAA shell of the JP (Figure 3a,b and Figure S3a,b). The PS-coated side of the PAA/PS-JP is hydrophobic, and PS does not swell upon immersing the particles in water. On the other hand, the PAA-coated side is hydrophilic, and PAA swells in water. The swelling range of PAA is between pH 4 and pH 10. However, a complete swelling is expected in the pH range from 7 to 10. The modification of JPs was conducted in deionized water at a pH value of 7−8, because of the triethylamine addition. The swelling/deswelling of polymers has led to an intercalation of metal ions within the hydrophilic polymer (PAA), which is also influenced by the incorporated carboxylic acid groups acting as a linking moiety.[32]

Cryo-TEM images of the corresponding samples revealed the distribution of NPs in the PAA polymer shell (Figure 3c and Figures S3c and S4). At pH 7−8, the PAA chains are stretched out, and therefore the NPs are adsorbed throughout the length of the polymer chains. Because of their amphiphilicity, the JPs sometimes assemble in clusters in water, and it could be clearly seen that they face each other with their PS sides (hydrophobic attractions), leaving the metal NPs in the PAA shell on the outer contour of the clusters (Figure S4a−c). When visualizing single particles, selective functionalization of the JP with the metal NPs could again be observed (Figure 3c and Figure S4d).

DOI: 10.1021/acsami.5b05224
ACS Appl. Mater. Interfaces 2015, 7, 21218−21225

DLS measurements of the PAA/PS-Ag-JP catalyst system at different pH values revealed the stimuli-responsive behavior of the PAA brush (Figure S5). At pH 2, aggregation of the particles is observed due to the collapsed state of the PAA chains. The situation completely changes starting from pH 7, at which the PAA polymer is fully swollen, therefore preventing the aggregation of the JPs due to electrostatic and steric effects. At pH 10 the same tendency to form single particles instead of aggregates is observed. The results correlate perfectly with the stimuli-responsive behavior of JPs without the adsorbed NPs.[23] Thus, the immobilized Ag nanoparticles do not hinder the stimuli-responsive behavior of the PAA brush, and the polymer provides a good distribution of the metallic NPs throughout its chains when in a swollen state (as confirmed by the cryo-TEM measurements, Figure 3c and Figure S4).

The role of the polymers is crucial in our hybrid Janus catalysts. The catalytic species (Ag or Au NPs) are specifically located in the hydrophilic hemisphere of the JP. The hydrophilic PAA thus provides a very good distribution of the nanoparticles in its chains, which swell upon immersion in water. Such distribution prevents the metal NPs from aggregation and provides better substance transport to the catalyst. In addition, PAA is a stimuli-responsive polymer, and its stimuli-responsive behavior could be further used for a precise control of the catalytic activity of our catalyst. Hydrophobic PS, on the other hand, provides the JPs with a high contrast in hydrophobicity at their opposite sides (advancing water contact angle on PAA-modified substrates is 58 ± 2°; receding contact angle, 14 ± 2°; on PS, 100 ± 2° and 77 ± 2°, respectively), which makes them perfect candidates for emulsion stabilization in interfacial catalysis.

EDX analysis of the PAA/PS-Ag-JP and PAA/PS-Au-JP samples was performed in order to confirm the chemical composition of the metal NPs (Figure 4 and Figure S6). In the case of PAA/PS-Ag-JP, EDX mapping of silver revealed a contrast in places, where the NPs were adsorbed (Figure 4). The spectrum of area 1 shows a clear Ag signal. In the case of PAA/PS-Au-JP, EDX mapping of gold revealed a contrast of Au, where the NPs were adsorbed (Figure S6). The gold signal in case of the PAA/PS-Ag-JP comes from the TEM grid, as gold TEM grids with a carbon film were used for the experiments.

Moreover, TEM analysis of NPs was performed in order to confirm their crystal structure (Figure S7). High-resolution TEM images at high magnifications revealed atomic layers in the corresponding NPs indicating their crystal structure. Diffraction patterns of the NPs contain reflexes characteristic for a fcc lattice typical for both silver and gold.

Further, we have prepared emulsions stabilized either by the PAA/PS-Ag-JP catalyst system or by reference PAA-modified fully covered (PAA FC) particles (Figure 5) at pH = 7. Photographs directly after emulsion preparation show that the emulsion stabilized by the homogeneously decorated PAA FC particles already started to disintegrate, revealing a phase separation between the oil and the water (Figure 5a). On the other hand, the emulsion stabilized by the Janus PAA/PS-Ag-JP catalyst remained stable. Light microscopy images of the emulsion show that the emulsion droplets in the case of PAA FC are much bigger if compared to the homogeneously distributed small droplets in the case of PAA/PS-Ag-JP Janus-based system (Figure 5b). These results indicate that the developed Janus JP-NP catalyst is perfectly suitable for emulsion stabilization and therefore for the future use in interfacial catalytic reactions. Addition of acidic solution (pH = 2) leads to rapid destabilization of emulsion with JPs that appear in formation of layered structure and the increase of size of the droplets (Figure 5c). The emulsion is destabilized at pH = 2 because PAA is in the less hydrophilic not-dissociated form.

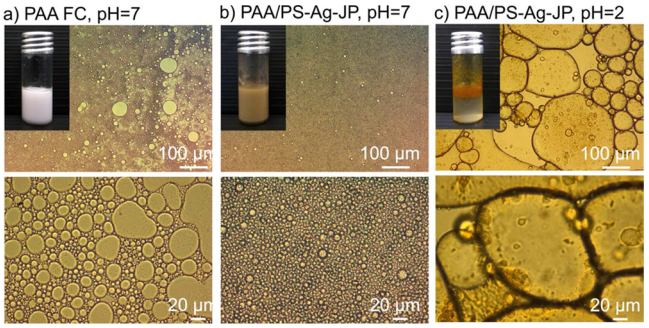

Figure 5. Representative photographs and light microscopy images at different magnifications of the emulsions prepared with fully covered PAA-modified 200 nm large particles at pH 7 (a), and the Janus PAA/PS-Ag-JP (b, c) catalyst system at pH 7 (b) and pH 2 (c).

Catalytic Reduction of Dyes. To investigate the accessibility of the immobilized metal nanoparticles, the reduction of two different dyes (Methylene Blue = MB, Eosin Y = EOY) as convenient benchmark systems was applied. For instance, a schematic illustration of the Methylene Blue catalytic reduction is shown in Figure 6a. In a typical procedure, a 10^{-5} M aqueous solution of the respective dye was mixed with a freshly prepared 0.1 M sodium borohydride solution and stirred for 1 min. Afterward, 0.25 mL of the respective Janus particle suspension (0.33 mg of particles) were added, and then samples were taken at 30 s (60 s for EOY) intervals and analyzed by UV−vis spectroscopy. The natural logarithm of the observed absorbance was plotted over the elapsed time. After linear fitting, the specific k values were accessible from the slope of the obtained regression curve. Regarding the obtained results, a complete reduction was observed for both dyes (Figure 6b−d and Figure S8). The difference between the obtained k values for MB (0.017 s^{-1}) and EOY (0.42 s^{-1}) can be explained by the interaction of the acidic PAA matrix and deprotonated dye functionalities. Regarding the logarithmic plot for the Eosin Y experiment, an initiation phase was observed (Figure 6d). We suppose that the diffusion of EOY through the PAA matrix takes longer than for MB, since interactions between the acidic PAA and the deprotonated groups of EOY are possible. Therefore, the rate constants were only determined in the linear region. In comparison, MB does not show a similar behavior, which means the reduction process of MB starts from the very beginning of the reaction. Furthermore, the decomposition of the herein reported systems is tremendously increased compared to silver nanoparticles deposited on, for example, plain silica spheres.[33]

The catalytic reduction of 4-nitrophenol was conducted in a similar manner as described above (reduction experiments with dyes), with the only difference being that these experiments were carried out at a higher temperature (40 °C). A successful reduction of 4-nitrophenol was observed for the Au-functionalized JPs (Figure 6e and Figure S8). The observed k value of this reaction (k_{app} = 0.101 s^{-1}) must be considered as apparent, since the concentration of sodium borohydride has an influence on k (as described in ref 34). Therefore, comparison with other systems, for example, bimetallic nanoparticles[35] or Au particles deposited on ceria[36] is difficult. Nevertheless, the observed k_{app}

DOI: 10.1021/acsami.5b05224
ACS Appl. Mater. Interfaces 2015, 7, 21218−21225

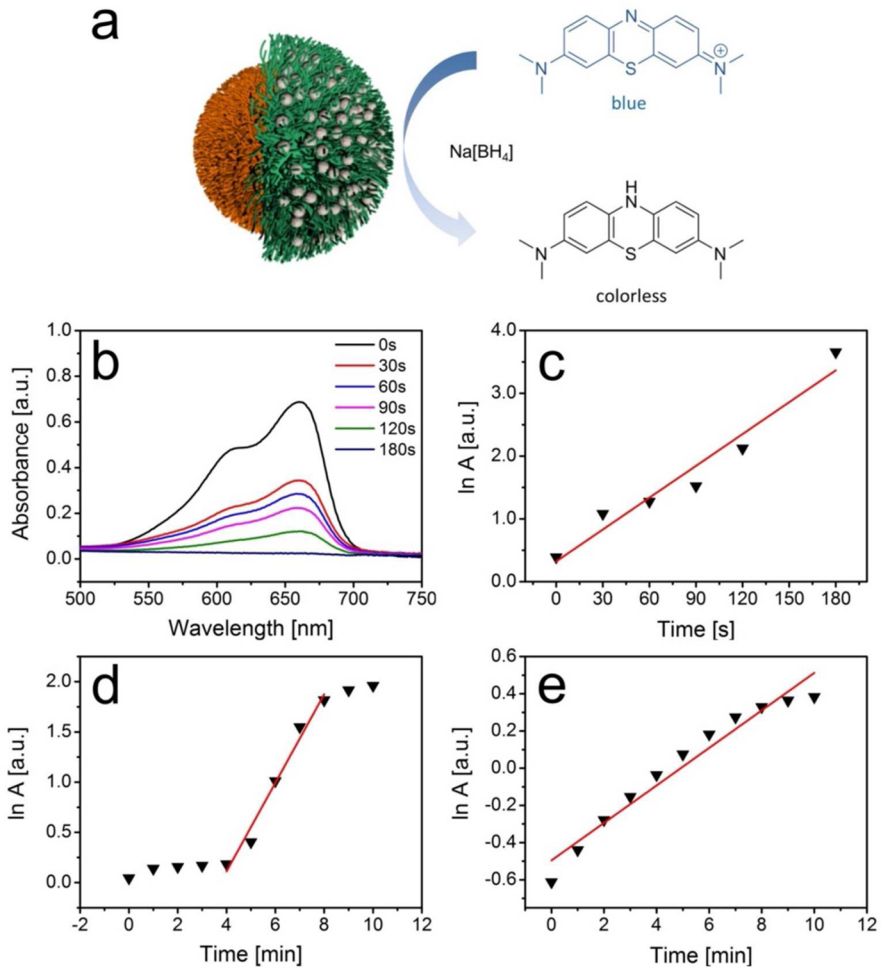

Figure 6. (a) Schematic illustration of the catalytic Methylene Blue reduction with sodium borohydride in the presence of Ag NP-modified PAA/PS-JP; (b) UV−vis spectra of the catalytic Methylene Blue reduction; logarithmic plots of the decreasing absorbance over elapsed time for the catalytic reduction of Methylene Blue (c) and Eosin Y (d) in the presence of Ag NP-modified PAA/PS-JP; (e) logarithmic plot of the decreasing absorbance over elapsed time for 4-nitrophenol reduction catalyzed by Au nanoparticle-functionalized PAA/PS-JP.

value is somewhat smaller than for the reported systems; however, the reduction takes place with smaller amounts of the catalyst.

Finally we demonstrated a combination of ability of PAA/PS-Ag-JP to stabilize emulsion and catalyze reduction of dyes (Figure 7). We prepared water−oil emulsion stabilized by PAA/PS-Ag-JP, which contained Eosin Y dye. The emulsion has red color because of dye and was stable (Figure 7a). The addition of $NaBH_4$ led to rapid disappearance of the red color because of the reduction of the dye. Moreover, the emulsion was destabilized (Figure 7b) and the pH of emulsion became around 10. We neutralized excess of $NaBH_4$ by acid to get pH = 6 and re-emulsified again by ultrasonication. The formed emulsion was stable (Figure 7c). At the end, we centrifuged the emulsion (Figure 7d) and got separate layers of water and oil (Figure 7e). The PAA/PS-Ag-JP precipitated at the bottom of the tube and at the interface between liquid phases that demonstrated possibility of recovery of JPs.

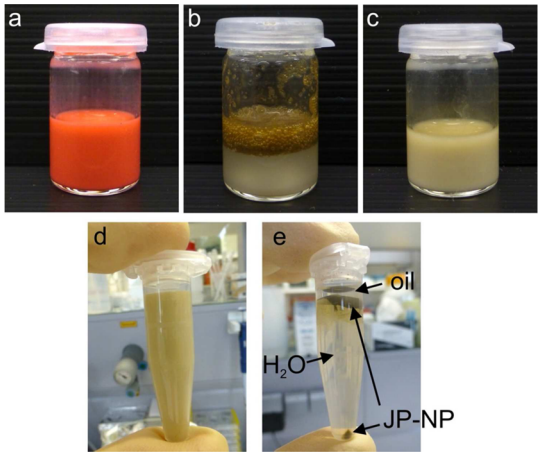

Figure 7. Reduction of Eosin Y in emulsion stabilized by PAA/PS-Ag-JP: photographs of (a) water−oil emulsion stabilized by PAA/PS-Ag-JPs and containing Eosin Y; (b) the same emulsion after addition of $NaBH_4$ and 10 min of incubation; (c and d) redisposed emulsion at pH = 6 after reduction of Eosin Y; (e) emulsion from d after centrifugation.

4. CONCLUSIONS

Within this study a novel type of hairy hybrid Janus catalyst, comprised of a silica core along with two types of polymer shells on its opposite sides (hydrophilic PAA and hydrophobic PS), has been designed. We have demonstrated successful selective functionalization of such amphiphilic Janus particles with either Ag or Au nanoparticles, which could be achieved in

DOI: 10.1021/acsami.5b05224
ACS Appl. Mater. Interfaces 2015, 7, 21218−21225

a straightforward manner. As a result, the catalytic species were localized selectively in the hydrophilic PAA-covered hemisphere of the hairy Janus particles, which was confirmed by EDX, TEM, and cryo-TEM analysis. The synthesized JPs with incorporated metallic nanoparticles demonstrated high interfacial activity and efficient stabilization of water−oil emulsions that can be tuned by pH. Furthermore, the accessibility of Ag and Au NPs was demonstrated by applying convenient benchmark reactions like the reduction of Methylene Blue, Eosin Y, and 4-nitrophenol. Ultimately, a successful and effective reduction of two dyes and a nitro compound with extremely low amounts of catalyst was conducted. Finally, we demonstrated that JPs are particularly promising for interfacial catalysis. Thus, the big advantages of the use of JPs with immobilized metallic nanoparticles are that (i) JPs effectively stabilize emulsions, (ii) the emulsion can be destabilized by utilizing responsive properties of the JPs, and (iii) JPs can easily be recovered after reaction and reused again.

In further experiments other stabilizing agents will be introduced, which will allow an incorporation of different nanoparticles, such as palladium, onto the Janus particles, and the respective modified Janus particle catalysts will be tested in *C,C* cross-coupling reactions.

■ ASSOCIATED CONTENT

Supporting Information

The Supporting Information is available free of charge on the ACS Publications website at DOI: 10.1021/acsami.5b05224.

Plasmon resonance bands of the NP-functionalized PAA/PS-JP, particle size distribution of the NPs, more representative TEM and cryo-TEM images of the Ag- or Au-functionalized PAA/PS-JP, EDX analysis of PAA/PS-Au-JP, HRTEM images as well as corresponding diffraction patterns of Ag and Au NPs, and UV−vis spectra of the catalytic 4-nitrophenol reduction with the Au NP-functionalized PAA/PS-JP (PDF)

■ AUTHOR INFORMATION

Corresponding Authors

*E-mail: heinrich.lang@chemie.tu-chemnitz. Phone: +49 (0) 371-531-21210. Fax: +49 (0)371-531-21219.
*E-mail: synytska@ipfdd.de. Phone: +49 (0351) 4658 327. Fax: +49 (0351) 4658 474.

Author Contributions

The manuscript was written through contributions of all authors. All authors have given approval to the final version of the manuscript.

Notes

The authors declare no competing financial interest.

■ ACKNOWLEDGMENTS

The authors thank Dr. Peter Formanek for the EDX measurements. A.S. received funding from the DFG Grant SY 125/4-1. C.S., A.J., and H.L. received funding from the DFG Grant FOR 1497. A.K. and G.S. received funding from IPF (Leibniz-Institut für Polymerforschung Dresden e.V).

■ REFERENCES

(1) Fang, X.; Zhai, T.; Gautam, U. K.; Li, L.; Wu, L.; Bando, Y.; Golberg, D. ZnS Nanostructures: From Synthesis to Applications. *Prog. Mater. Sci.* **2011**, *56*, 175−287.

(2) Lei, Y.; Yang, S.; Wu, M.; Wilde, G. Surface Patterning Using Templates: Concept, Properties and Device Applications. *Chem. Soc. Rev.* **2011**, *40*, 1247−1258.

(3) Yang, S.; Guo, F.; Kiraly, B.; Mao, X.; Lu, M.; Leong, K. W.; Huang, T. J. Microfluidic Synthesis of Multifunctional Janus Particles for Biomedical Applications. *Lab Chip* **2012**, *12*, 2097−2102.

(4) Resasco, D. E. Carbon Nanohybrids Used as Catalysts and Emulsifiers for Reactions in Biphasic Aqueous/Organic Systems. *Chin. J. Catal.* **2014**, *35*, 798−806.

(5) Chen, Q.; Bae, S. C.; Granick, S. Directed Self-Assembly of a Colloidal Kagome Lattice. *Nature* **2011**, *469*, 381−384.

(6) Hwang, S.; Lahann, J. Differentially Degradable Janus Particles for Controlled Release Applications. *Macromol. Rapid Commun.* **2012**, *33*, 1178−1183.

(7) Crowley, J. M.; Sheridon, N. K.; Romano, L. Dipole Moments of Gyricon Balls. *J. Electrost.* **2002**, *55*, 247−259.

(8) Ruhland, T. M.; Lang, J. R. V.; Alt, H. G.; Müller, A. H. E. Magnetic Core-Shell Nanoparticles as Carriers for Olefin Dimerization Catalysts. *Eur. J. Inorg. Chem.* **2013**, *2013*, 2146−2153.

(9) He, J.; Liu, Y.; Hood, T. C.; Zhang, P.; Gong, J.; Nie, Z. Asymmetric Organic/Metal(Oxide) Hybrid Nanoparticles: Synthesis and Applications. *Nanoscale* **2013**, *5*, 5151−5166.

(10) Seh, Z. W.; Liu, S.; Zhang, S. Y.; Bharathi, M. S.; Ramanarayan, H.; Low, M.; Shah, K. W.; Zhang, Y. W.; Han, M. Y. Anisotropic Growth of Titania onto Various Gold Nanostructures: Synthesis, Theoretical Understanding, and Optimization for Catalysis. *Angew. Chem., Int. Ed.* **2011**, *50*, 10140−10143.

(11) Hu, J.; Zhou, S.; Sun, Y.; Fang, X.; Wu, L. Fabrication, Properties and Applications of Janus Particles. *Chem. Soc. Rev.* **2012**, *41*, 4356−4378.

(12) Wang, C.; Yin, H.; Dai, S.; Sun, S. A General Approach to Noble Metal−Metal Oxide Dumbbell Nanoparticles and Their Catalytic Application for CO Oxidation. *Chem. Mater.* **2010**, *22*, 3277−3282.

(13) Rodríguez-Fernández, D.; Liz-Marzán, L. M. Metallic Janus and Patchy Particles. *Part. Part. Syst. Charact.* **2013**, *30*, 46−60.

(14) Pradhan, S.; Ghosh, D.; Chen, S. Janus Nanostructures Based on Au-TiO_2 Heterodimers and Their Photocatalytic Activity in the Oxidation of Methanol. *ACS Appl. Mater. Interfaces* **2009**, *1*, 2060−2065.

(15) Seh, Z. W.; Liu, S.; Low, M.; Zhang, S. Y.; Liu, Z.; Mlayah, A.; Han, M. Y. Janus Au-TiO_2 Photocatalysts with Strong Localization of Plasmonic Near-Fields for Efficient Visible-Light Hydrogen Generation. *Adv. Mater.* **2012**, *24*, 2310−2314.

(16) Binks, B. P.; Fletcher, P. D. I. Particles Adsorbed at the Oil−Water Interface: A Theoretical Comparison between Spheres of Uniform Wettability and "Janus" Particles. *Langmuir* **2001**, *17*, 4708−4710.

(17) Walther, A.; Hoffmann, M.; Muller, A. H. Emulsion Polymerization Using Janus Particles as Stabilizers. *Angew. Chem., Int. Ed.* **2008**, *47*, 711−714.

(18) Crossley, S.; Faria, J.; Shen, M.; Resasco, D. E. Solid Nanoparticles that Catalyze Biofuel Upgrade Reactions at the Water/Oil Interface. *Science* **2010**, *327*, 68−72.

(19) Faria, J.; Ruiz, M. P.; Resasco, D. E. Phase-Selective Catalysis in Emulsions Stabilized by Janus Silica-Nanoparticles. *Adv. Synth. Catal.* **2010**, *352*, 2359−2364.

(20) Lv, W.; Lee, K. J.; Li, J.; Park, T. H.; Hwang, S.; Hart, A. J.; Zhang, F.; Lahann, J. Anisotropic Janus Catalysts for Spatially Controlled Chemical Reactions. *Small* **2012**, *8*, 3116−3122.

(21) Kirillova, A.; Stoychev, G.; Ionov, L.; Eichhorn, K. J.; Malanin, M.; Synytska, A. Platelet Janus Particles with Hairy Polymer Shells for Multifunctional Materials. *ACS Appl. Mater. Interfaces* **2014**, *6*, 13106−13114.

(22) Stöber, W.; Fink, A.; Bohn, E. Controlled Growth of Monodisperse Silica Spheres in the Micron Size Range. *J. Colloid Interface Sci.* **1968**, *26*, 62−69.

(23) Berger, S.; Synytska, A.; Ionov, L.; Eichhorn, K.-J.; Stamm, M. Stimuli-Responsive Bicomponent Polymer Janus Particles by "Grafting

DOI: 10.1021/acsami.5b05224
ACS Appl. Mater. Interfaces 2015, 7, 21218−21225

from"/"Grafting to" Approaches. *Macromolecules* **2008**, *41*, 9669−9676.
(24) Berger, S.; Ionov, L.; Synytska, A. Engineering of Ultra-Hydrophobic Functional Coatings Using Controlled Aggregation of Bicomponent Core/Shell Janus Particles. *Adv. Funct. Mater.* **2011**, *21*, 2338−2344.
(25) Kirillova, A.; Stoychev, G.; Ionov, L.; Synytska, A. Self-Assembly Behavior of Hairy Colloidal Particles with Different Architectures: Mixed versus Janus. *Langmuir* **2014**, *30*, 12765−12774.
(26) Kelly, K. L.; Coronado, E.; Zhao, L. L.; Schatz, G. C. The Optical Properties of Metal Nanoparticles: The Influence of Size, Shape, and Dielectric Environment. *J. Phys. Chem. B* **2003**, *107*, 668−677.
(27) Steffan, M.; Jakob, A.; Claus, P.; Lang, H. Silica Supported Silver Nanoparticles from a Silver(I) Carboxylate: Highly Active Catalyst for Regioselective Hydrogenation. *Catal. Commun.* **2009**, *10*, 437−441.
(28) Tuchscherer, A.; Schaarschmidt, D.; Schulze, S.; Hietschold, M.; Lang, H. Gold Nanoparticles Generated by Thermolysis of ″All-in-One″ Gold(I) Carboxylate Complexes. *Dalton Trans.* **2012**, *41*, 2738−2746.
(29) Tuchscherer, A.; Schaarschmidt, D.; Schulze, S.; Hietschold, M.; Lang, H. Simple and Efficient: Gold Nanoparticles from Triphenylphosphane Gold(I) Carboxylates without Addition of any Further Stabilizing and Reducing Agent. *Inorg. Chem. Commun.* **2011**, *14*, 676−678.
(30) Lu, Y.; Spyra, P.; Mei, Y.; Ballauff, M.; Pich, A. Composite Hydrogels: Robust Carriers for Catalytic Nanoparticles. *Macromol. Chem. Phys.* **2007**, *208*, 254−261.
(31) Huang, Q.; Shen, W.; Xu, Q.; Tan, R.; Song, W. Properties of Polyacrylic Acid-Coated Silver Nanoparticle Ink for Inkjet Printing Conductive Tracks on Paper With High Conductivity. *Mater. Chem. Phys.* **2014**, *147*, 550−556.
(32) Love, J. C.; Estroff, L. A.; Kriebel, J. K.; Nuzzo, R. G.; Whitesides, G. M. Self-Assembled Monolayers of Thiolates on Metals as a Form of Nanotechnology. *Chem. Rev.* **2005**, *105*, 1103−1170.
(33) Jiang, Z.-J.; Liu, C.-Y.; Sun, L.-W. Catalytic Properties of Silver Nanoparticles Supported on Silica Spheres. *J. Phys. Chem. B* **2005**, *109*, 1730−1735.
(34) Wunder, S.; Lu, Y.; Albrecht, M.; Ballauff, M. Catalytic Activity of Faceted Gold Nanoparticles Studied by a Model Reaction: Evidence for Substrate-Induced Surface Restructuring. *ACS Catal.* **2011**, *1*, 908−916.
(35) Cui, J.; Gao, L.; Yan, S.; Zhang, W.; Li, Y.; Gao, L. The Direct Decomposition of Nitric Oxide Over Fe/CNOs (CNOs: Carbon Nano Onions). *Synth. React. Inorg., Met.-Org., Nano-Met. Chem.* **2015**, *45*, 158−163.
(36) Pozun, Z. D.; Rodenbusch, S. E.; Keller, E.; Tran, K.; Tang, W.; Stevenson, K. J.; Henkelman, G. A Systematic Investigation of p-Nitrophenol Reduction by Bimetallic Dendrimer Encapsulated Nanoparticles. *J. Phys. Chem. C* **2013**, *117*, 7598−7604.

DOI: 10.1021/acsami.5b05224
ACS Appl. Mater. Interfaces 2015, 7, 21218−21225